

Ultra-low-dose CBCT: new cornerstone of paranasal sinus imaging*

Pekka Tamminen^{1,2,3,5,6}, Jorma Järnstedt⁴, Jura Numminen¹, Antti Lehtinen⁴,
Lauri Lehtimäki^{5,6}, Markus Rautiainen^{1,6}, Ilkka Kivekäs^{1,6}

Rhinology 61: 3, 221 - 230, 2023

<https://doi.org/10.4193/Rhin22.385>

¹ Department of Otorhinolaryngology – Head and Neck Surgery, Tampere University Hospital, Tampere, Finland

² Department of Otorhinolaryngology, Satasairaala, Pori, Finland

³ Department of Internal Medicine, Tampere University Hospital, Tampere, Finland

⁴ Medical Imaging Centre, Department of Radiology Tampere University Hospital, Tampere, Finland.

⁵ Allergy Centre, Tampere University Hospital, Tampere, Finland

⁶ Faculty of Medicine and Health Technology, Tampere University, Tampere, Finland

***Received for publication:**

October 21, 2022

Accepted: January 12, 2023

Abstract

Background: This study evaluates the clinical image quality (IQ) and usability of a sinonasal ultra-low-dose (ULD) cone-beam computed tomography (CBCT) scan. The results are compared to those of a high resolution (HR) CBCT scan to identify the strengths and weaknesses of a ULD CBCT protocol.

Methodology: Sixty-six anatomical sites in 33 subjects were imaged twice using two imaging modalities: HR CBCT (Scanora 3Dx scanner; Soredex, Tuusula, Finland) and ULD CBCT (Promax 3D Mid scanner; Plandent, Helsinki, Finland). IQ, opacification and obstruction, structural features and operative usability were assessed.

Results: The overall IQ in subjects with “no or minor opacification” was excellent: 100% (HR CBCT) and 99% (ULD CBCT) of ratings were evaluated as sufficient for every structure. Increased opacification reduced the quality of both imaging modalities, resulting in sufficient IQ in 97% (HR CBCT) and 92% (ULD CBCT) of evaluations. With greater opacification, the sufficient–insufficient ratio was better ($p < 0.05$) for HR CBCT regarding the anterior ethmoidal artery, lateral lamella, frontal recess, cribriform plate, superior concha and posterior ethmoidal artery. ULD CBCT’s operative applicability was generally good with moderate restraints in frontoethmoidectomy, frontal sinusotomy, sphenotomy and posterior ethmoidectomy in cases with greater opacification.

Conclusions: IQ of paranasal ULD CBCT is sufficient for clinical diagnostics and should be considered for surgical planning. We recommend it as the primary imaging protocol for all patients who meet imaging criteria due to recurrent or chronic nasal symptoms. Additional or conventional imaging might be needed for patients with extensive chronic rhinosinusitis and/or indications of frontal sinus involvement.

Key words: Cone beam computed tomography (CBCT), paranasal sinuses, sinusitis, radiation dosage, nasal surgical procedures

Introduction

Imaging of paranasal sinuses is required to obtain information on mucosal areas in the upper airways that cannot be reached by endoscopy. It also provides a view of the structure of the bone and of the relationship of anatomical structures and pathways when surgical intervention is planned.

Annually, a mean of 95 surgical procedures per 100 000 inhabitants were conducted on nose and paranasal sinuses (in which

preoperative imaging is presumed) in Finland during 2014–2018⁽¹⁾. The annual mean for computed tomography scans of the paranasal region/upper airways was 131 scans per 100 000 inhabitants, of which 35% (range 32–36%) were imaged with cone-beam computed tomography (CBCT) devices and the remainder with multi-slice computed tomography (MSCT) devices⁽¹⁾. The equivalent count for magnetic resonance imaging was only 14 annual scans per 100 000 inhabitants⁽¹⁾, most of which were likely taken alongside CT for additional soft tissue visualization.

Oral and maxillofacial CBCT devices became commercially available in 1996 in Europe and in 2001 in the USA ⁽²⁾. The image is taken with a two-dimensional detector that rotates around the object from 180° to 360° ⁽³⁾. Most of the images are captured with the patient sitting upright with a stabilizing head support. It is space-saving but does not fully prevent motion artefacts ⁽³⁻⁵⁾. The image data consist of small isotropic 3D units, or voxels, that represent the degree of X-ray absorption at each location ⁽³⁾. The size of the voxel determines the image resolution, and the resulting image can be rendered and re-rendered freely. CBCT has multiple applications in otorhinolaryngology, the most common being imaging of the sinonasal cavities, but its usage should be broadened ⁽⁶⁾.

The radiation burden is substantially lower with CBCT compared to MSCT ⁽⁷⁻¹²⁾. In the first well-conducted and comprehensive cadaver study, midface MSCT and CBCT provided similar bone imaging performance, while CBCT produced better image quality (IQ), less noise and equal resolution at low-dose settings ⁽⁷⁾. De Cock et al. ⁽⁸⁾ showed that high-resolution (HR) CBCT and MSCT are equally suitable for evaluating sinonasal polyposis and that the opacification of paranasal sinuses reduces the IQ of both modalities. However, they did not use the images of the same subjects in the evaluation. If soft tissue assessment is needed due to trauma, complication, or other reason, MSCT should be preferred ^(7,9). Abduwani et al. ⁽¹⁰⁾ and Han et al. ⁽¹¹⁾ compared consecutive MSCT and HR CBCT images of the same subjects, but with interventions in between. The clinically relevant results were presented only with sample images ⁽¹⁰⁾ or evaluated with a binary outcome (presence or absence) for a limited number of anatomical structures ⁽¹¹⁾ without knowledge of the degree of opacification.

Güldner et al. ⁽¹²⁾ published a comparison of HR CBCT vs low-dose (LD) CBCT with approximately 150 subjects in each group. Irradiation was halved with LD CBCT, and the evaluated overall IQ was equal, but there was only one rater and the groups comprised different subjects. A recent technical phantom study compared the capabilities of two CBCT devices against MSCT, using three dose-neutral imaging protocols in each: ultra-low-dose (ULD), LD and default dose. The radiation dose reduction to default regarding CBCT was -86% in ULD and -65% in LD. All CBCT protocols had better resolution and minimal bone density Hounsfield unit error throughout the protocol scale, while MSCT excelled in contrast and uniformity ⁽¹³⁾. In summary, there are only a few studies (with varying quality) comparing the clinical usability of CBCT to that of MSCT and one technical study of ULD CBCT.

Our aims were to evaluate the clinical IQ and usability of a sinonasal ULD CBCT scan and to compare these to those of HR

CBCT to identify the strengths and weaknesses of this imaging modality.

Materials and methods

Thirty-three subjects were imaged twice using two different imaging modalities: HR CBCT and ULD CBCT in this order. As each anatomical structure were evaluated separately on both sides (left and right) of the head, 66 comparisons between the modalities were available. The included subjects had chronic or recurrent rhinosinusitis, were not previously operated on in the nasal or paranasal area and were referred to the Department of Otorhinolaryngology at Tampere University Hospital (TAUH). The images were taken 4 to 6 weeks apart in accordance with the follow-up protocol of our ongoing study.

Imaging devices and specifications

The HR CBCT scans were obtained using a Scanora 3Dx scanner (Soredex, Tuusula, Finland) with the following specifications: field of view (FOV): 140 × 165 mm, 90 kV, 8 mA, scanning time: 4s, voxel size: 0.2 (high resolution), slice thickness: 1 mm, spacing: 1 mm, zoom: 1 and dose area product (DAP): 1725.85 mGycm².

The ULD CBCT scans were obtained using a Promax 3D Mid scanner (Plandent, Helsinki, Finland) with the following specifications: FOV: 160 × 170 mm, 120 kV, 2 mA, two scans stitched together by Romexis software, scanning time: 4.486 s and 4.522 s, voxel size: 0.6 (ultra-low-dose), slice thickness: 1.4 mm, spacing: 1.4 mm, zoom: 0.8 and DAP: 2 × 115 (=230) mGycm².

Standard axial, coronal and sagittal scans were reconstructed using a Philips IntelliSpace Portal v10.1.5.51377 workstation (Philips Medical Systems, the Netherlands). No enhancements were used. To maximize overall IQ, different reconstructions were chosen based on previous experience with ULD imaging. All the original and reconstructed slices were stored in the picture archiving and communication systems (PACS) of TAUH.

Methods and means of evaluation

Two ear, nose and throat (ENT) surgeons (JN and PT) evaluated the clinical information of the images such as opacification and obstruction, as well as features of accessory ostium, concha bullosa, insertion of uncinatus, anterior ethmoidal artery and lamina papyracea. The structures (aforementioned and those discussed later with IQ) were chosen according to our collective judgement to support the evaluation of operative range. Lateral lamella's length was chosen as it can be measured in every evaluation. It is also one of the important structures when considering complications of ethmoidectomy.

The data were divided into two groups according to the opaci-

Table 1. Image quality of named structures according to the degree of opacification. Sixty-six anatomical sites were imaged with two modalities and evaluated by four rates.

Structure	ULD CBCT								HR CBCT							
	No or minor opacification [§] , (one-sided score 0-2; n= 132 - 136 [¶])								More opacification [§] , (one-sided score 3-25; n= 120 - 128 [¶])							
	Likert scale				Sufficient [#]				Likert scale				Sufficient [#]			
	5	4	3	2	1	0	%	p-value	5	4	3	2	1	0	%	p-value
Maxillary Sinus	16	101	18	0	0	0	100	1 ¹	10	88	27	2	0	0	98	0.498 ¹
	<u>130</u>	<u>6</u>	0	0	0	0	100		<u>117</u>	<u>9</u>	0	0	0	0	100	
Infundibulum	21	98	16	0	0	0	100	1 ¹	8	65	41	7	3	3	90	0.052 ²
	<u>118</u>	<u>17</u>	<u>1</u>	0	0	0	100		<u>88</u>	<u>29</u>	<u>4</u>	<u>2</u>	0	<u>3</u>	96	
Bulla Ethmoidalis	23	101	12	0	0	0	100	1 ¹	9	71	40	8	0	0	94	0.603 ²
	<u>128</u>	<u>8</u>	0	0	0	0	100		<u>96</u>	<u>22</u>	<u>2</u>	<u>6</u>	0	0	95	
Middle Concha	13	107	16	0	0	0	100	1 ¹	4	81	39	4	0	0	97	0.748 ¹
	<u>127</u>	<u>8</u>	0	0	0	0	100		<u>100</u>	<u>18</u>	<u>3</u>	<u>5</u>	0	0	96	
Lamina Papyracea	11	110	15	0	0	0	100	1 ¹	4	89	31	4	0	0	97	0.684 ¹
	<u>128</u>	<u>8</u>	0	0	0	0	100		<u>106</u>	<u>16</u>	<u>2</u>	<u>2</u>	0	0	98	
Anterior Ethmoidal Artery	12	109	12	2	0	1	98	0.247 ¹	6	71	41	9	0	1	92	0.006 ²
	<u>128</u>	<u>8</u>	0	0	0	0	100		<u>105</u>	<u>16</u>	<u>4</u>	0	0	<u>1</u>	99	
Lateral Lamella	12	102	16	2	0	0	98	0.243 ¹	6	51	51	17	0	0	86	<0.001 ²
	<u>122</u>	<u>13</u>	0	0	0	0	100		<u>86</u>	<u>31</u>	<u>7</u>	0	<u>2</u>	0	98	
Frontal Recess	29	87	18	0	0	0	100	1 ¹	8	47	52	18	0	2	84	0.005 ²
	<u>124</u>	<u>11</u>	0	0	0	0	100		<u>79</u>	<u>33</u>	<u>6</u>	<u>2</u>	<u>2</u>	<u>2</u>	95	
Cribriform Plate	22	98	15	1	0	0	99	1 ¹	6	68	24	19	5	6	77	0.009 ²
	<u>126</u>	<u>10</u>	0	0	0	0	100		<u>71</u>	<u>29</u>	<u>12</u>	<u>9</u>	0	<u>5</u>	89	
Superior Concha	12	108	13	3	0	0	98	0.247 ¹	6	78	28	16	0	0	88	<0.001 ²
	<u>124</u>	<u>12</u>	0	0	0	0	100		<u>96</u>	<u>18</u>	<u>10</u>	<u>2</u>	0	0	98	
Posterior Ethmoidal Artery	6	99	25	0	0	6	96	0.030 ¹	4	65	50	5	0	4	93	0.033 ²
	<u>124</u>	<u>12</u>	0	0	0	0	100		<u>98</u>	<u>19</u>	<u>7</u>	0	0	<u>2</u>	98	
Planum sphenoidale	12	107	17	0	0	0	100	0.498 ¹	8	92	26	2	0	0	98	0.445 ¹
	<u>104</u>	<u>26</u>	<u>4</u>	<u>2</u>	0	0	99		<u>84</u>	<u>33</u>	<u>5</u>	<u>4</u>	0	0	97	
Optic nerve	12	109	14	1	0	0	99	1 ¹	6	92	28	2	0	0	98	0.498 ¹
	<u>130</u>	<u>6</u>	0	0	0	0	100		<u>110</u>	<u>14</u>	<u>2</u>	0	0	0	100	
Carotid Artery	4	116	14	2	0	0	99	0.498 ¹	3	88	27	2	0	0	98	0.237 ¹
	<u>126</u>	<u>10</u>	0	0	0	0	100		<u>110</u>	<u>12</u>	<u>4</u>	0	0	0	100	
Sphenoethmoidal Recess	12	112	12	0	0	0	100	1 ¹	6	82	34	4	2	0	95	0.161 ¹
	<u>130</u>	<u>6</u>	0	0	0	0	100		<u>103</u>	<u>17</u>	<u>4</u>	<u>2</u>	0	0	98	
Sphenoid Sinus	22	101	13	0	0	0	100	1 ¹	7	91	25	2	0	2	97	0.715 ¹
	<u>127</u>	<u>6</u>	0	0	0	0	100		<u>107</u>	<u>13</u>	<u>2</u>	0	0	<u>3</u>	98	
Total							99	<0.001 ^{1,3}							92	<0.001 ^{1,3}
							<u>100</u>								<u>97</u>	

Ultra-low-dose cone-beam computed tomography (ULD CBCT); high resolution cone-beam computed tomography (HR CBCT); ¹ Fishers Exact Test, ² Chi-square (Pearson), ³ Bonferroni corrected p-value<0.05/16; [§] Median opacification and obstruction are presented in Table 3; [¶] Maximum count of individual evaluations of a structure was 528 (66 structures, two modalities, both opacification groups and four raters). Row sum produces the exact n. [#] Sufficient includes Likert scale grades from five to three; The level of significance was set at p<0.05 (indicated with bold font).



Figure 1. The minor difference in image quality does not alter the diagnostic confidence or identification of a structure. Sagittal, coronal and axial plane images of paranasal sinuses without opacification from both modalities: row A was produced by HR CBCT and row B by ULD CBCT.

fication score of the first scan (HR CBCT), since the opacification of pneumatized paranasal sinuses and the nasal cavity is known to have an impact on differentiation of structures and on IQ. The Zinreich modified Lund–Mackay score was utilized⁽¹⁴⁾. It rates sinuses from 0 to 5 according to opacification (0 = 0%; 1 = 1–25%; 2 = 26–50%; 3 = 51–75%; 4 = 76–99%; 5 = 100%) and ostia from 0 to 1 (0 = no obstruction; 0.5 = partial or suspected obstruction; 1 = total or definitive obstruction). Each side was scored independently with the following ranges: sinuses (maxillary, ethmoidal anterior and posterior, sphenoidal, frontal) 0–25 points and ostia (middle meatus, infundibulum, frontal and sphenoidal recesses) 0–4 points. The threshold of 3 points on a single side was used to split the data: from 0 to 2 to the category “minor or no opacification” and from 3 upwards to “more opacification”. The cut-off value was set to mimic the Lund–Mackay score 2 or less (~8% of total score)⁽¹⁵⁾.

Four raters (AL, JJ, JN and PT) including two radiologists and two ENT-surgeons, with clinical experience as specialists of between 6 and 23 years, assessed the IQ of every anatomical structure on both sides of each subject separately using a Sectra IDS7 PACS workstation and a Barco MXRT 4700 Dicom monitor with a resolution of 2560 × 1600 (60 Hz). All scans were recoded with a random, unique number from 1 to 1000 and rearranged in ascending order. The image metadata (including name and modality)

were hidden, and fixed planes (axial, coronal and sagittal) were used. The sharpness of the images could be adjusted freely. The IQ for every anatomical site in each image was rated using a Likert scale from 0 to 5: 0 = cannot be assessed; 1 = poor IQ; 2 = reduced IQ; 3 = acceptable IQ; 4 = good IQ; and 5 = excellent IQ. Ratings from 0 to 2 were considered as insufficient, and ratings from 3 to 5 were considered sufficient for anatomical guidance and for preoperative decisions. The threshold is in accordance with “as low as diagnostically acceptable” principle, pursuing to reduce radiation doses⁽¹⁶⁾.

The ENT surgeons also estimated whether the IQ and information were sufficient to guide surgical procedures such as frontoethmoidectomy, frontal sinusotomy, posterior ethmoidectomy, sphenotomy, uncinectomy, middle meatal antrostomy, or partial anterior ethmoidectomy. A 3-point scale was used: “yes”, “yes, with restraints” or “no, essential structures are not visible”. The surgical procedures were chosen to cover the maximal extent of typical endoscopic operation, done due to chronic rhinosinusitis.

Sample size

Sample size was based on an 80% power with an alpha-error of 5% to find a between-modality difference of 10 percentage points (98 % vs. 88 %) in the proportion of evaluations with suffi-

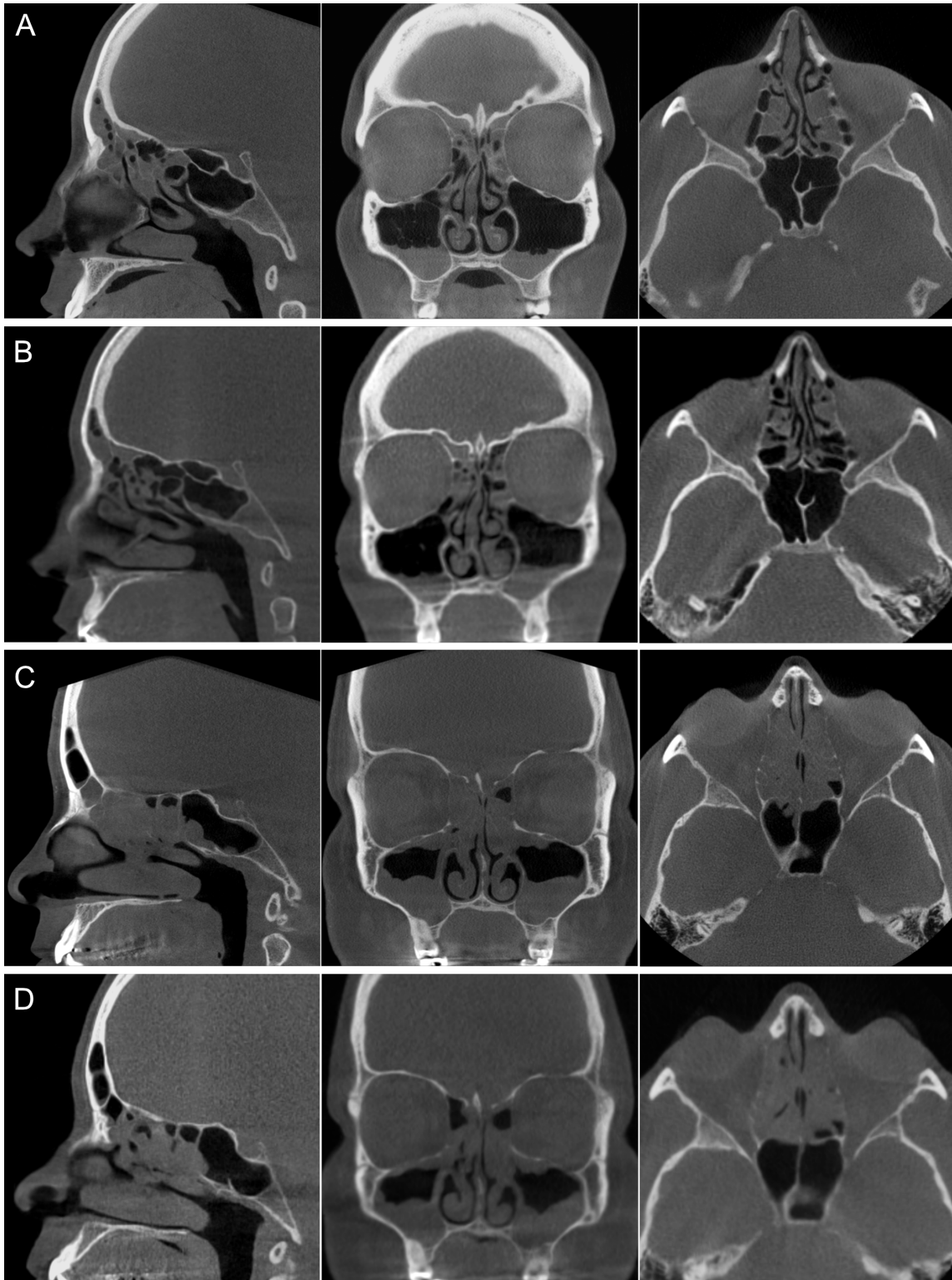


Figure 2. Increased opacification affects the in image quality of an individual structure differently, creating possible limitations to some surgical procedures. Sagittal, coronal and axial plane images of paranasal sinuses with greater opacification. The image quality of rows A (HR CBCT) and B (ULD DBCT) was rated among the highest and that of rows C (HR CBCT) and D (ULD CBCT) the lowest.

cient IQ. Thus, the needed number of evaluations is at least 120.

Statistical analysis

The statistical analysis was conducted using SPSS Statistics 27.0.1.0 (International Business Machines Corporation [IBM],

Table 2. Likert scale from 0 to 5 was used to assess the image quality of HR CBCT and ULD CBCT images.

	Structure	Quality
0	Cannot be assessed	No identifiable structure or other reason
1	Poor image quality	Some anatomic resemblance
2	Reduced image quality	Poorly defined anatomic details
3*	Acceptable image quality	Limitations in anatomic detail
4	Good image quality	Clear anatomic details
5	Excellent image quality	Distinct anatomic details

* If an overall understanding of the structures anatomy was received, the grade was three or more, if not, grade two, one or zero was given. Exemplary questions to guide the rating: Can the course of the structure be followed? Can thin bony walls/structures be identified?

Armonk, USA). Cohen’s Kappa was used to assess inter-rater agreement for two raters and a nominal variable. Kappa values increasingly greater than zero represent increasing better-than-chance agreement for the two raters. A maximum value of +1 indicates perfect agreement. Fisher’s exact test (two-tailed) or chi-squared (Pearson) were used for cross-classifiable results. To compare continuous data, the related-samples Wilcoxon test or paired samples T-test were used according to the normality of the data (Shapiro–Wilk test).

Ethical statement

The study was approved by the TAUH ethics committee (R17011) and registered at clinicaltrials.gov (NCT04171167), and all patients provided written informed consent. Repetitive imaging was conducted ethically; the additional radiation burden was equivalent to a two days of background radiation.

Results

Sixty-six anatomical sites in 33 subjects, imaged twice using two different imaging modalities, yielded a maximum of 132 evaluations for a single studied item from one rater. The two imaging modalities had similar opacification and obstruction scores in both opacification groups (Table 3). However, in subjects with minor opacification only, the opacification score was slightly but not clinically significantly higher in HR CBCT images. The groups are considered comparable with no significant changes in disease burden between the images.

Regardless of the degree of opacification, 99% of the IQ ratings were categorized as sufficient when imaged with HR CBCT and 96% with ULD CBCT (Table 1). The overall IQ in the “no or minor opacification” group was excellent: on average, 100% of HR CBCT and 99% of ULD CBCT ratings were evaluated as sufficient in every structure. Increased opacification reduced the IQ of both imaging modalities, and ULD CBCT suffered slightly more. The proportions of sufficient IQ in the “more opacification” group were 97% with HR CBCT and 92% with ULD CBCT.

Cribriform plate had sufficient IQ in 89% of the ratings, with all other evaluated structures scoring at least 95% with HR CBCT. The maxillary sinus, middle concha, lamina papyracea, planum sphenoidale, optic nerve, carotid artery, sphenothmoidal recess and sphenoid sinus received the “sufficient” rating in at least 95% of the evaluations with ULD CBCT. Infundibulum, bulla ethmoidalis, anterior ethmoidal artery, lateral lamella, frontal recess, cribriform plate, superior concha and posterior ethmoidal artery images were rated as clinically sufficient in 77% to 94% of the evaluations.

In the “no or minor opacification” group, the sufficient–insufficient ratio of IQ was better for HR CBCT regarding the posterior ethmoidal artery, but equal between the modalities for all other structures (Table 1) In the “more opacification” group, this ratio was better for HR CBCT regarding the anterior ethmoidal artery, lateral lamella, frontal recess, cribriform plate, superior concha and posterior ethmoidal artery.

The measured length of the lateral lamella was equal when comparing ULD CBCT and HR CBCT within the groups (Table 3).

There was moderate to excellent inter-rater agreement regarding the features of lamina papyracea and concha bullosa (Table 4). Some amount of variance occurred in the results regarding the accessory ostium. The rater assessments of insertion of uncinatus were mingled, whereas for the anterior ethmoidal artery the effect of increased opacification was seen in decreased inter-rater agreement.

Applicability for surgical operations

Uncinectomy, middle meatal antrostomy and partial anterior ethmoidectomy were operations that could have been performed based on every scan in the dataset.

Sphenotomy and posterior ethmoidectomy had 2 and 2 “with restraints” answers (out of 62) with HR CBCT and 6 and 8 (out

Table 3. The degree of opacification and obstruction in subgroups and the length of lateral lamella. Sixty-six anatomical sites were imaged with two modalities and evaluated by two ENT surgeons.

	No or minor opacification, (one-sided score 0-2)			More opacification, (one-sided score 3-25)		
	ULD CBCT	HR CBCT	p-value	ULD CBCT	HR CBCT	p-value
n of evaluations	68	68		64	64	
Opacification Score	1 [0–2]	1 [1–2]	< 0.001*	6 [4–9]	6 [4–9]	0.305*
Obstruction Score	0.0 [0.0–0.0]	0.0 [0.0–0.0]	0.330*	1.8 [1.0–3.0]	1.5 [0.0–2.9]	0.114*
Length of lateral lamella (mm)	4.35 (SD 0.92)	4.16 (SD 0.86)	0.082 [†]	3.89 (SD 0.98) ¹	3.69 (SD 0.86) ²	0.179 [†]

Ultra-low-dose cone-beam computed tomography (ULD CBCT), high resolution cone-beam computed tomography (HR CBCT); * Related-samples Wilcoxon test; [†] Paired samples T-test; ¹ n=63; ² n=60; Maximum row count of individual evaluations was 264 (66 evaluated items, two modalities, both opacification groups and two raters).

of 64) with ULD CBCT within the “more opacification” group, respectively. Frontoethmoidectomy and frontal sinusotomy based on ULD CBCT in the “more opacification” group received the most reserved answers and variation: 42 (66%) “yes”, 20 (31%) “with restraints” and 2 (3%) “no, essential structures are not visible”. There were two (3 %) “with restraints” and two (3 %) “no” – answers, respectively, even with HR CBCT.

In the “no or minor opacification” group frontoethmoidectomy and frontal sinusotomy were the only to receive two (3 %) “with restraints” answers, with every other procedure being feasible.

Image samples

The ULD CBCT image was softer, but it did not alter the diagnostic confidence or identification of a structure (Figure 1). With increased opacification the IQ of some individual structures may suffer more, with no clinically relevant reduction in overall diagnostic or operative confidence (Figure 2, panels A and B). Depending on surgeons’ preferences some, but not all, operations from our described range might be limited (Figure 2, panels C and D).

Discussion

We found that ULD CBCT image quality and clinical/operative usability were excellent in cases with minor paranasal and nasal mucosal pathology (Figure 1). IQ and clinical/operative usability decreased slightly more with ULD CBCT imaging modality compared to HR CBCT when more opacification was encountered yet remained excellent with HR CBCT and good with ULD CBCT (Figure 2). The IQ reduction result is in line with the results of de Cock et al. ⁽⁸⁾. The closest comparable clinical study, that of Güldner et al. ⁽¹²⁾, showed equal IQ of LD CBCT to HR CBCT, but they presumably assessed only paranasal sinuses with minor mucosal findings. To our knowledge this is the first imaging comparison with a ULD CBCT patient cohort.

Although our sample does not include every consecutive patient who was referred to our hospital and met the inclusion criteria, it represents typical cases that are imaged during the process of clinical evaluation of bothersome nasal symptoms. Recurrent and chronic upper respiratory tract symptoms are very common in developed countries, but their relation to degree of opacification is weak ⁽¹⁷⁾. Chronic rhinosinusitis affects 5–12% of the general population ⁽¹⁵⁾. With cases of visible nasal polyposis, the pathology is reliably witnessed already in anterior rhinoscopy. Most patients, on the other hand, have varying ranges of subjective symptoms and scant objective findings, thus necessitating imaging for objective evaluation. Furthermore, early imaging might be cost effective ⁽¹⁸⁾. Half of the subjects in this study had a total opacification score of 0 to 4 with the median score for ostium obstruction being 0. These patients typically have, for example, harmless maxillary sinus cysts or transient mucosal reaction due to common cold, allergens or irritants. Our results suggest that conservative and even operative treatment can be planned and executed based on the initial ULD CBCT imaging in at least nine out of ten new patients.

Increased opacification lowers the IQ by shifting the grey values or creating artefacts ^(19,20). The contrast of the image is dependent on the distribution and number of densities inside the field of view ⁽¹⁹⁾. Another adverse factor of IQ is the erosion of the thin bony walls within thickened or polypous mucosa ⁽²¹⁾. Arbitrary factors like mucus can also disturb the visualization of ostia or an accessory ostium. Therefore, it is essential to evaluate the same subject with no interventions or changes in pathology between images when imaging modalities are compared. Ideally, all scans should be taken at the same instant, but this is routinely possible only with cadavers. In our results, the weak point of HR CBCT with greater opacification was the cribriform plate, with 89% of evaluations exhibiting sufficient quality. The skull base area has been found to be prone to HR CBCT-related

Table 4. The features of a structure and inter-rater agreement. Sixty-six anatomical sites were imaged with two modalities and evaluated by two ENT surgeons.

<i>ULD CBCT</i>		No or minor opacification [§] , (one-sided score 0-2)					More opacification [§] , (one-sided score 3-25)					
<i>HR CBCT</i>												
Structure	Exists	Suspected	Non-existent	Cannot be assessed	Total	Inter-rater agreement Cohen's Kappa (p-value)	Exists	Suspected	Non-existent	Cannot be assessed	Total	Inter-rater agreement Cohen's Kappa (p-value)
Accessory ostium	8	6	54	0	68	0.167 (0.168)	12	4	44	4	64	0.431 (< 0.001)
	<u>14</u>	<u>3</u>	<u>49</u>	<u>2</u>	<u>68</u>	0.665 (< 0.001)	<u>10</u>	<u>2</u>	<u>44</u>	<u>6</u>	<u>62</u>	0.312 (0.005)
	Exists, pneumatized	Exists, opacified	Non-existent				Exists, pneumatized	Exists, opacified	Non-existent			
Concha bullosa	26	0	42	0	68	0.638 (< 0.001)	13	1	49	1	64	0.667 (< 0.001)
	<u>20</u>	<u>0</u>	<u>48</u>	<u>0</u>	<u>68</u>	0.721 (< 0.001)	<u>17</u>	<u>4</u>	<u>40</u>	<u>1</u>	<u>62</u>	0.741 (< 0.001)
	Middle concha-ethmoidal	Lamina papyracea	Skull-base				Middle concha-ethmoidal	Lamina papyracea	Skull-base			
Insertion of uncinatus	42	19	7	0	68	0.053 (0.145)	25	12	1	26	64	0.280 (< 0.001)
	<u>39</u>	<u>21</u>	<u>4</u>	<u>3</u>	<u>67</u>	<u>0.004 (0.959)</u>	<u>28</u>	<u>16</u>	<u>1</u>	<u>17</u>	<u>62</u>	<u>0.130 (0.074)</u>
	In contact with skull-base	Hanging partly from skullbase	Hanging from skull-base				In contact with skullbase	Hanging partly from skullbase	Hanging from skull-base			
Anterior Ethmoidal Artery	47	1	20	0	68	0.798 (< 0.001)	39	10	11	4	64	0.246 (0.026)
	<u>42</u>	<u>7</u>	<u>19</u>	<u>0</u>	<u>68</u>	0.617 (< 0.001)	<u>36</u>	<u>17</u>	<u>9</u>	<u>0</u>	<u>62</u>	0.335 (0.002)
	Course evident	Course uncertain					Course evident	Course uncertain				
Lamina Papyracea	68	0		0	68	*	60	4		0	64	0.475 (0.002)
	<u>67</u>	<u>0</u>		<u>0</u>	<u>67</u>	<u>*</u>	<u>62</u>	<u>0</u>		<u>0</u>	<u>62</u>	<u>*</u>

Ultra-low-dose conebeam computed tomography (ULD CBCT), high resolution conebeam computed tomography (HR CBCT); *Cohen's Kappa cannot be computed; [§] Median opacification and obstruction are presented in Table 3; Maximum count of individual evaluations of a structure was 264 (66 structures, two modalities, both opacification groups and two raters). The level of significance was set at p<0.05 (indicated with bold font).

technical artefacts: edge gradient effect (at high contrast sharp edges), ring artefacts and increased noise level (5,19,20). Anterior and frontoethmoidal (infundibulum, bulla ethmoidalis, anterior ethmoidal artery and frontal recess) as well as skull base-related structures (lateral lamella, cribriform plate, superior concha, and posterior ethmoidal artery) were those that received the most "insufficient" IQ ratings in ULD CBCT. The results are in line with the increased "with restraints" and "no" answers of ULD CBCT scans' operative applicability. Though the IQ of the first operative landmarks (infundibulum and bulla ethmoidalis) was decreased in ULD CBCT images, it should be noted that the suffi-

cient-insufficient ratio of IQ was not significantly different when compared to HR CBCT. In addition, the measured average length of the lateral lamella was identical in ULD CBCT and HR CBCT in both groups. However, the clinical and operative usability of the scans should always be judged as an entity and in relation to the clinical question (as demonstrated in Image samples and in Applicability for surgical operations), not solely by the p-values of the IQ.

The current European position paper on rhinosinusitis and nasal polyps 2020 (15), emphasizes MSCT as the gold standard of sino-

nasal imaging, but it acknowledges its LD modalities and CBCT as well. The transition from MSCT to CBCT in sinonasal imaging began years ago, and CBCT is now in wide clinical use, but relatively few studies have been published⁽⁷⁻¹²⁾. In our institution, 95% of paranasal sinus imaging is done with CBCT (unpublished own data). Default resolution of CBCT is at its best in fine bone structure imaging, such as for teeth and paranasal sinuses⁽¹³⁾. The inferiority of soft tissue visibility in CBCT compared to MSCT is not an issue in “common case” imaging of paranasal sinuses. Incidental pathological findings are rare in imaging of rhinosinusitis⁽⁹⁾: CBCT imaging (theoretically produced) would miss 3.3% of the soft tissue findings that are visible in the scans conducted with MSCT, but only one third of them would be previously unknown⁽⁹⁾. A technical IQ comparison of ULD, LD and default protocols of CBCT and MSCT⁽¹³⁾ provides a suggestive background to our study: all CBCT protocols produced better resolution and more concise grey values of bone. Lower radiation doses worsened expectedly the measured results of all devices⁽¹³⁾, but as shown the technical analysis and comparison of images and methods might be misleading for example due to inconsistent changes of grey values⁽¹⁹⁾. We bring a clinical aspect to the conversation with our real-world patient cohort, the scans of which were used for treatment planning.

Regarding surgical treatment, we tried ULD CBCT scans successfully in our intraoperative navigation system (Fusion ENT Navigation System, Medtronic, Minneapolis, USA) during an actual operation as well. Since it was not our objective, we do not have any data to provide details on this. Nevertheless, the notice is certainly something requiring further study.

Due to our study design, we do not have the effective radiation doses for these scanners in this imaging area. The published mean effective doses are 0.119 mSv for paranasal CBCT⁽²²⁾ and 0.6 mSv for paranasal MSCT⁽²³⁾, being equivalent to 2 and 9 weeks of background radiation, respectively. The effective dose for facial scans with the Scanora 3Dx (HR CBCT device) is 0.104 mSv (unpublished data from the manufacturer; measured in the University Hospital of Oulu, Finland, in 2013, according to the dosimetric principles of the Finnish Radiation and Nuclear Safety Authority [STUK]). For facial imaging with the Promax 3D Mid ULD (ULD CBCT device), the dose is 0.018 mSv (FOV: 200 × 170 mm) (published in a poster; ID 0920, 2015 IADR/AADR/CADR General Session, Boston Massachusetts), which equals to 2 days of background radiation. Thus, the ULD CBCT uses one sixth or one seventh of the radiation of HR CBCT. For further reference, the effective dose for one projection single-plane X-ray of paranasal sinuses or lung is 0.03 mSv, equivalent to 3 days of background radiation⁽²⁴⁾.

We need to develop our imaging protocols towards lesser radi-

ation exposure to patients⁽¹⁶⁾, but also prove that new methods are clinically valid and applicable. There is growing epidemiological evidence that CT scans can cause cancer, especially after childhood exposure⁽²⁵⁾. Shifting from the use of MSCT to CBCT (HR or even ULD) whenever possible would greatly diminish the count of 85/100 000 annual MSCT scans nationally⁽¹⁾ and the radiation burden. We have managed to implement the shift in our institution, as 95% of sinonasal imaging is nowadays CBCT, thus contradicting the national data (35%). It is also the reason why MSCT imaging is not included in this study. ULD CBCT modality is in clinical use in increasing numbers, encouraged by this study.

Our study's greatest strengths are, firstly, its real patient cohort in which the same subjects were repetitively imaged with no interventions in the interim, and secondly, the images were intended for and used in clinical decision making. The 4–6 week gap between images could have been even shorter, however. Additionally, the scans were viewed and rated in random order and without information about the patients or imaging modalities by four specialists, and clinical as well as operative aspects were included. No technical evaluation or comparison of the images was made, though this accompanied our objective. Finally, although we had one group with little or no opacification and a second with greater opacification, the overall burden of paranasal sinus pathology might be less than in some other institutes. This must be considered when considering generalisation of our results and their applicability.

Conclusion

We found that the IQ of paranasal ULD CBCT is sufficient for clinical diagnostics and should be considered for surgical planning. Therefore, we recommend ULD CBCT as the primary imaging protocol for all patients who meet the imaging criteria due to recurrent or chronic nasal symptoms. It should also be considered when repetitive imaging is needed. With ULD CBCT's good image quality, three-dimensional view and minute radiation exposure, there is no justifiable indication for conventional two-dimensional imaging of the paranasal sinuses if ULD CBCT is reasonably available. ULD CBCT is widely applicable also in secondary and tertiary care units, but patients with extensive chronic rhinosinusitis and/or indications of frontal sinus involvement are still likely to require an additional higher-dose imaging protocol or further advancements in ULD protocols and hardware.

Acknowledgements

The authors would like to thank study nurses Piitu Oksanen and Merja Rumpunen for patient management and guidance. The authors would also like to thank statistician Mika Helminen from Tampere University for his advice on statistical analysis.

Authorship contribution

PT: Conceptualization, Investigation, Methodology, Formal analysis, Data Curation, Writing Original Draft, Review & Editing, Project administration. JJ: Conceptualization, Investigation, Writing Original Draft, Review & Editing. JN: Conceptualization, Investigation, Writing Review & Editing, Supervision. AL: Investigation, Writing Review & Editing. LL: Conceptualization, Methodology, Formal analysis, Writing Original Draft, Review & Editing, Supervision, Project administration, Funding acquisition. MR: Conceptualization, Methodology, Writing Review & Editing, Supervision, Project administration, Funding acquisition. IK: Conceptualization, Methodology, Formal analysis, Writing Original Draft, Review & Editing, Supervision, Project administration.

Conflict of interest

The authors have no conflicts of interest regarding the manuscript.

Funding

This work was supported by funding from Tampere Tuberculosis Foundation; Research Foundation of the Pulmonary Diseases; Competitive State Research Financing of the Expert Responsibility area of Tampere University Hospital; Tampere University Hospital Support Foundation; The Finnish ORL-HNS Foundation. Funders did not have any role in any part of the study.

References

1. The Finnish Institute for Health and Welfare - Sampo registry [Internet]. <https://sampo.thl.fi/>. Available from: https://sampo.thl.fi/pivot/prod/fi/thil/perus01/fact_thil_perus01.
2. Miracle AC, Mukherji SK. Conebeam CT of the head and neck, part 2: Clinical applications. *Am J Neuroradiol.* 2009;30:1285–92.
3. Pauwels R, Araki K, Siewerdsen JH, Thongvigitmanee SS. Technical aspects of dental CBCT: State of the art. *Dentomaxillofacial Radiol.* 2015;44.
4. Spin-Neto R, Matzen LH, Hermann L, de Carvalho e Silva Fuglsig JM, Wenzel A. Head motion and perception of discomfort by young children during simulated CBCT examinations. *Dentomaxillofacial Radiol.* 2021;50(3):20200445.
5. Schulze R, Heil U, Groß D, et al. Artefacts in CBCT: A review. *Dentomaxillofacial Radiol.* 2011;40: 265–73.
6. Tamminen P, Järnstedt J, Lehtinen A, et al. Ultra-low-dose CBCT scan: rational map for ear surgery. *Eur Arch Otorhinolaryngol.* 2023;280(3):1161–1168.
7. Veldhoen S, Schöllchen M, Hanken H, et al. Performance of cone-beam computed tomography and multidetector computed tomography in diagnostic imaging of the midface: A comparative study on Phantom and cadaver head scans. *Eur Radiol.* 2017;27:790–800.
8. de Cock J, Zanca F, Canning J, Pauwels R, Hermans R. A comparative study for image quality and radiation dose of a cone beam computed tomography scanner and a multislice computed tomography scanner for paranasal sinus imaging. *Eur Radiol.* 2015;25:1891–900.
9. Fakhraan S, Alhilali L, Sreedher G, et al. Comparison of simulated cone beam computed tomography to conventional helical computed tomography for imaging of rhinosinusitis. *Laryngoscope.* 2014;124:2002–6.
10. al Abduwani J, Zilinskiene L, Colley S, Ahmed S. Cone beam CT paranasal sinuses versus standard multidetector and low dose multidetector CT studies. *Am J Otolaryngol - Head Neck Med Surg.* 2016;37:59–64.
11. Han M, Kim HJ, Choi JW, Park DY, Han JG. Diagnostic usefulness of cone-beam computed tomography versus multi-detector computed tomography for sinonasal structure evaluation. *Laryngoscope Investig Otolaryngol.* 2022;7:662–70.
12. Güldner C, Diogo I, Leicht J, et al. Reduction of Radiation Dosage in Visualization of Paranasal Sinuses in Daily Routine. *Int J Otolaryngol.* 2017;2017:1–5.
13. Ronkainen AP, Al-Gburi A, Liimatainen T, Matikka H. A dose-neutral image quality comparison of different CBCT and CT systems using paranasal sinus imaging protocols and phantoms. *Eur Arch Oto-Rhino-Laryngol.* 2022;279:4407–14.
14. Zinreich SJ. Imaging for staging of rhinosinusitis. *Ann Otol Rhinol Laryngol Suppl.* 2004;193:19–23.
15. Fokkens WJ, Lund VJ, Hopkins C, et al. European Position Paper on Rhinosinusitis and Nasal Polyps 2020. *Rhinology.* 2020;1–464.
16. Jaju PP, Jaju SP. Cone-beam computed tomography: Time to move from ALARA to ALADA. *Imaging Sci Dent.* 2015;45:263–5.
17. Valtonen O, Bizaki A, Kivekäs I, Rautiainen M. Three-Dimensional Volumetric Evaluation of the Maxillary Sinuses in Chronic Rhinosinusitis Surgery. *Ann Otol Rhinol Laryngol.* 2018;127:931–6.
18. Leung RM, Chandra RK, Kern RC, Conley DB, Tan BK. Primary care and upfront computed tomography scanning in the diagnosis of chronic rhinosinusitis: a cost-based decision analysis. *Laryngoscope.* 2014;124:12–8.
19. Pauwels R, Jacobs R, Singer SR, Mupparapu M. CBCT-based bone quality assessment: Are Hounsfield units applicable? *Dentomaxillofacial Radiol.* 2015;44.
20. Kuusisto N, Vallittu PK, Lassila LVJ, Huuomonen S. Evaluation of intensity of artefacts in CBCT by radio-opacity of composite simulation models of implants in vitro. *Dentomaxillofacial Radiol.* 2015;44: 2):20140157.
21. Siddiqui J, Millard R, Eweiss AZ, Beale T, Lund VJ. Sinonasal bony changes in nasal polyposis: Prevalence and relationship to disease severity. *J Laryngol Otol.* 2013;127:755–9.
22. Nardi C, Salerno S, Molteni R, et al. Radiation dose in non-dental cone beam CT applications: a systematic review. *Radiologia Medica.* 2018;123:765–77.
23. Lin EC. Radiation risk from medical imaging. *Mayo Clinic Proc.* 2010;85:1142–6.
24. Radiation and Nuclear Safety Authority. Radiation doses of radiographic examinations [Internet]. <https://www.stuk.fi/web/en/topics/use-of-radiation-in-health-care/radiographic-examinations/radiation-doses-of-radiographic-examinations>.
25. Berrington A, Gonzalez DE, Pasqual E, Veiga L. Epidemiological studies of CT scans and cancer risk: the state of the science. 2021. *Br J Radiol.* 2021;94:20210471.

Pekka Tamminen
Tampere University Hospital
Elämäntie 2
33520 Tampere
Finland

E-mail: pekka.tamminen@tuni.fi

ORCID:

PT: 0000-0003-2139-6457
 JJ: 0000-0003-1503-3078
 JN: 0000-0003-4211-4244
 AL: 0000-0001-8305-4650
 LL: 0000-0003-1586-4998
 MR: 0000-0002-5905-0059
 IK: 0000-0002-6931-3641